Broadband Theoretical Gyroelectric Junction Circulator Tracking Behavior at 77 K

Robin Sloan, *Member, IEEE,* Chin K. Yong, and Lionel E. Davis, *Fellow, IEEE*

***Abstract*—The perfect circulation conditions for the gyroelectric circulator are given for a gyroelectric ratio with magnitude in the range zero to two. Values of this ratio above unity given in this paper correspond to the frequency regions where the effective permittivity is negative. The subsequent Green's function analysis employs the modified Bessel function. In accordance with the Drude model of semiconductors, a theoretical low-loss GaAs design is presented with a 20 dB isolation bandwidth of approximately 90% at an operating temperature of 77 K. The theoretical broadband circulation tracking behavior of this design is demonstrated for gyroelectric ratios which may exceed a magnitude of unity. The operating frequency range for this particular circulator design is below the extraordinary wave resonance frequency. In order to measure the microwave properties of the magnetised semiconductor disk, a two port analysis is performed based upon the Drude model of semiconductors.**

I. Introduction

BROADBAND operation of the ferrite junction circulator is limited to upper frequencies of around 40 GHz due to the maximum saturation magnetization of the ferrite materials available. Wu and Rosenbaum [1] showed that by carefully choosing a surrounding dielectric medium and inserting a ferrite puck of a set radius and coupling angle, a broadband gyromagnetic circulator can be designed. The tracking between the perfect circulation conditions and the calculated variations with gyromagnetic ratio, κ/μ, was illustrated for values in the range $0.5 < \kappa/\mu < 1$. To increase the frequency performance still further Schloemann and Blight [2] considered the case where the effective permeability, μ_{eff}, is negative. The analysis of this case yields a Green's function involving the modified Bessel function. In the ferrite case, such a frequency region is usually used to extend the bandwidth of a below resonance broadband circulator into the frequency range of $f < f_o + f_M$ where f_o is the natural processional frequency of the electrons and f_M is the magnetization frequency. Equally for the gyroelectric case, where the magnitude of the gyroelectric ratio κ/ε may be greater than unity over a broad range of frequencies, it is desirable to have design information available. This will increase the possible range of frequencies where tracking of the perfect circulation conditions is feasible.

In order to illustrate this point, the perfect circulation conditions are presented for the range $0 < |\kappa/\varepsilon| < 2$. The values of the gyroelectric ratio presented here between unity and two correspond to the frequencies where the effective permittivity ϵ_{eff} of the magnetized semiconductor medium is negative. There exists a frequency band between the cyclotron frequency, f_C, and the extraordinary wave resonance frequency f_{res} where the effective permittivity is positive and the gyroelectric ratio is greater than unity. The circulation solutions for this region are not considered in this paper. The Green's function analysis of the magnetized semiconductor disk at frequencies corresponding to evanescent propagation involves the modified Bessel functions.

A design of a slot-fed gallium arsenide (GaAs) circulator operating at 77 K from 50 GHz up to 125 GHz is reported. The tracking behavior of this device against the extended perfect circulation conditions is also demonstrated.

The designs mentioned in this paper require an accurate knowledge of the semiconductor properties according to the Drude model. In order to measure and compare these properties with expected values at microwave frequencies, a two-port semiconductor disk resonator was analyzed. S-parameter variations with applied magnetic field can be theoretically determined and will enable the disk properties to be calibrated by measurement. This information can then be used to validate the Drude model and consequently to provide necessary parameter values for the design of the actual semiconductor junction circulator.

II. The Green's Function with Modified Bessel Functions

The gyroelectric effect arises from the cyclotron motion of nearly free electrons according to the Drude model under the influence of an applied steady magnetic field. It can be expressed mathematically as a tensor relative permittivity [3]. The analysis of this permittivity tensor in Maxwell's equations with the assumption of a positive effective permittivity, ϵ_{eff}, was reported in papers [3] and [4] and the Green's function involves Bessel functions.

For a negative value of ϵ_{eff}, the Green's function is comprised of modified Bessel functions. In this case, the Helmholtz equation becomes

$$\frac{\partial^2 H_z}{\partial r^2} + \frac{1}{r}\frac{\partial H_z}{\partial r} + \frac{1}{r^2}\frac{\partial^2 H_z}{\partial \phi^2} - \overline{k}^2 H_z = 0 \tag{1}$$

where $\overline{k} = \omega\sqrt{\mu_o \epsilon_o |\epsilon_{eff}|}$ and the general solution of (1) for a realizable finite magnetic field at the center of the disk is

$$H_{z,n}(r, \phi) = b_n I_n(\overline{k}r)e^{jn\phi} \tag{2}$$

Manuscript received March 29, 1996. This work was supported by DRA Malvern, UK.

The authors are with the Department of Electrical Engineering and Electronics, University of Manchester Institute of Science and Technology, Manchester M60 1QD, U.K.

Publisher Item Identifier S 0018-9480(96)08573-0.

where n are integers, b_n are constants and I_n is the nth-order modified Bessel function of the first kind. In general, losses due to the electron collision frequency, v_c, will mean ϵ_{eff} is complex and so the Bessel functions will possess a complex argument.

The boundary conditions of Fig. 1 will determine the electric field E_ϕ at the disk edge ($r = R$). In this case E_ϕ will be zero apart from at the slotline ports. Bosma's analysis [5] can be applied here for negative ϵ_{eff} to produce the following Green's function

$$G(r,\, \phi;\, R,\, \phi') = \frac{j}{2\pi \overline{Z}_{\text{eff}}} \sum_{n=-\infty}^{n=+\infty} \cdot \frac{I_n(\overline{k}r)e^{jn(\phi-\phi')}}{I_n'(\overline{k}R) - \dfrac{\kappa}{\varepsilon} \cdot \dfrac{n}{\overline{k}R} \cdot I_n(\overline{k}R)} \tag{3}$$

where $\overline{Z}_{\text{eff}} = \sqrt{\mu_o/(\epsilon_o|\epsilon_{\text{eff}}|)}$ and is the effective wave impedance of the unbounded plasma.

To calculate the S-parameters of the magnetized semiconductor disk only the Green's function at the disk edge is required. The magnetic field H_z which is determined by the boundary condition confining E_ϕ is given by (4).

$$H_z(r,\, \phi) = \int_{-\pi}^{\pi} G(r,\, \phi; R,\, \phi') \cdot E_\phi(R,\, \phi')\, d\phi'. \tag{4}$$

Supposing E_ϕ at each port is constant over the aperture width, then only the Green's function is to be integrated. By adopting the notation $G(R,\, \phi;\, R,\, \phi') = G(\phi; \phi')$ and integrating for averaged H_z at those ports, the integrated Green's function will take the form of (5). The half angle subtended at each port is denoted by ψ

$$\overline{G}(\phi;\, \phi') = \frac{1}{2\psi} \int_{\phi-\psi}^{\phi+\psi} \int_{\phi'-\psi}^{\phi'+\psi} G(\phi;\, \phi')\, d\phi'\, d\phi. \tag{5}$$

Substituting (3) into (5) gives

$$\overline{G}(\phi;\, \phi') = \frac{j\psi I_0(\overline{x})}{\pi \overline{Z}_{eff} I_0'(\overline{x})} - \frac{2}{\pi \overline{Z}_{eff}} \sum_{n=1}^{n=\infty} \frac{\sin^2(n\psi)}{n^2\psi} \cdot \frac{\dfrac{\kappa}{\varepsilon}\dfrac{n}{\overline{x}} I_n^2(\overline{x}) \sin[n(\phi-\phi')] - jI_n(\overline{x})I_n'(\overline{x}) \cos[n(\phi-\phi')]}{[I_n'(\overline{x})]^2 - \left[\dfrac{\kappa}{\varepsilon}\dfrac{n}{\overline{x}} I_n(\overline{x})\right]^2} \tag{6}$$

where $\overline{x} = \overline{k}R$.

Using the integrated Green's function, the S-parameters of the ideal, lossless semiconductor junction circulators can be calculated [3]. For perfect circulation, one of the scattering elements S_{21} or S_{31} is zero and applying similar analysis to that reported by Wu and Rosenbaum [1], the principal solutions to the circulation equations are found.

III. Valid Region for the Modified Bessel Function Solutions

In order to discover the frequency ranges over which these solutions are valid, it is worthwhile considering the variation of κ/ε and ϵ_{eff} with frequency. These are depicted in Figs. 2 and 3. The frequencies at which $|\kappa/\varepsilon|$ equals to unity are marked

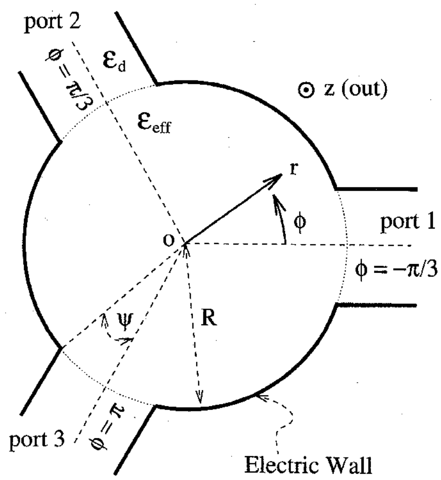

Fig. 1. Boundary conditions for the semiconductor junction circulator with slotline ports.

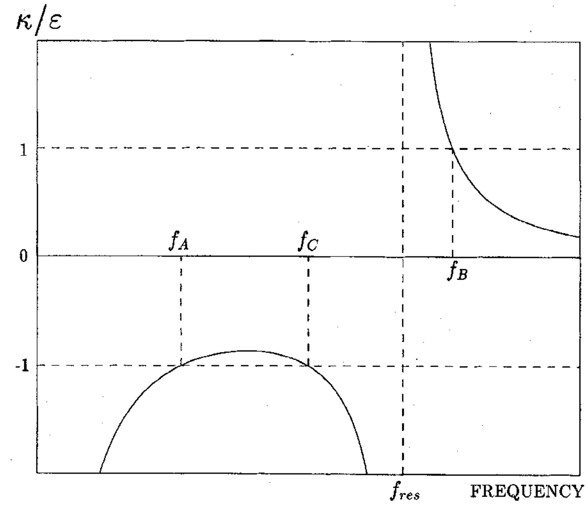

Fig. 2. Variation of the gyroelectric ratio of a semiconductor material with respect to frequency (lossless case).

as f_A, f_C and f_B where

$$f_A = \frac{f_C}{2}\left(\sqrt{1 + \frac{4f_p^2}{\epsilon_r f_C^2}} - 1\right) \tag{7}$$

$$f_B = \frac{f_C}{2}\left(\sqrt{1 + \frac{4f_p^2}{\epsilon_r f_C^2}} + 1\right) \tag{8}$$

and $f_p = (1/2\pi)\sqrt{Ne^2/m_e^*\epsilon_o}$ is the plasma frequency, and $f_B - f_A = f_C$. N and m_e^* are electron concentration and effective mass, respectively.

From Figs. 2 and 3, it can be seen that below the extraordinary wave resonance frequency $f_{res} = [f_C^2 + f_p^2/\epsilon_r]^{1/2}$ there are three regions of interest which require solutions. The first region is from dc to f_A where ϵ_{eff} is negative and $|\kappa/\varepsilon|$ is larger than unity, the second region is between f_A and f_C where ϵ_{eff} is positive and $|\kappa/\varepsilon|$ is less than unity, and the final is from f_C to f_{res} where ϵ_{eff} is positive but $|\kappa/\varepsilon|$ is greater than one. It should be noted that an equivalent behavior at frequencies below f_A, which is due to the existence of a plasma frequency, does not exist in ferrites.

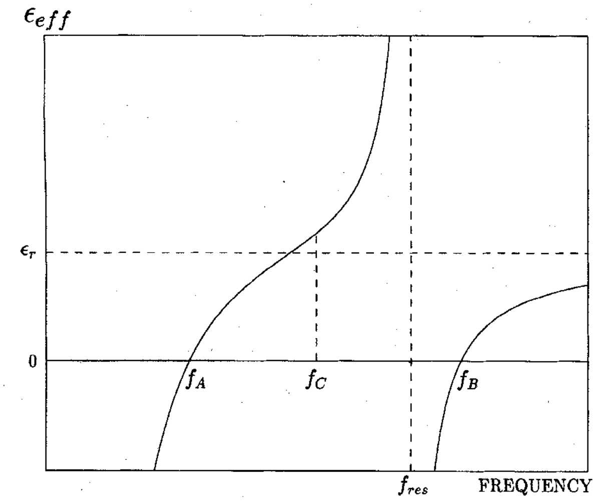

Fig. 3. Variation of the effective permittivity of a semiconductor material with respect to frequency (lossless case).

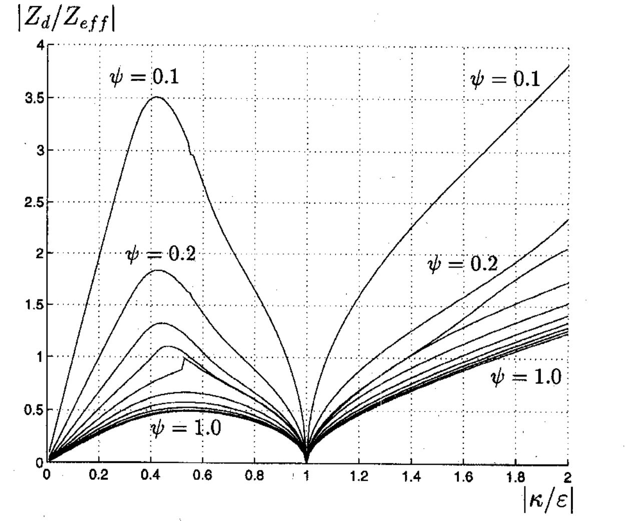

Fig. 5. The second perfect circulation condition corresponding to frequency regions where $0 < |\kappa/\varepsilon| < 1$ for $\epsilon_{\text{eff}} > 0$; and $1 < |\kappa/\varepsilon| < 2$ for $\epsilon_{\text{eff}} < 0$.

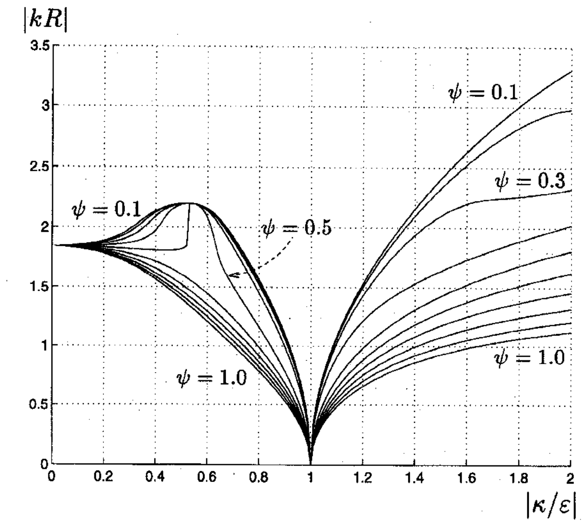

Fig. 4. The first perfect circulation condition corresponding to frequency regions where $0 < |\kappa/\varepsilon| < 1$ for $\epsilon_{\text{eff}} > 0$; and $1 < |\kappa/\varepsilon| < 2$ for $\epsilon_{\text{eff}} < 0$.

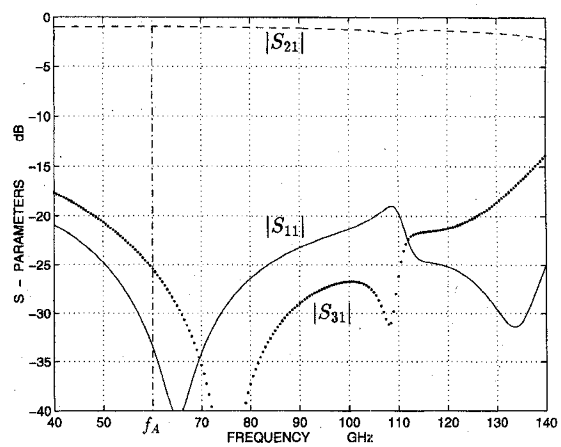

Fig. 6. The predicted performance of a GaAs junction circulator at 77 K with $R = 0.28$ mm, $\psi = 0.54$ rad, $\epsilon_d = 20$, $B_o = 0.6$ T, $f_{\text{res}} = 286$ GHz and $v_c = 1.3 \times 10^{11}$ s^{-1}.

Above the f_{res}, there are just two distinct frequency regions. Firstly, $|\kappa/\varepsilon| > 1$ and $\epsilon_{\text{eff}} < 0$ at frequencies between f_{res} and f_B and secondly, $|\kappa/\varepsilon| < 1$ and $\epsilon_{\text{eff}} > 0$ for frequencies greater than f_B.

The modified Bessel function solutions apply to the following frequency regions: *dc* to f_A and f_{res} to f_B. The curves considered here correspond to the ideal lossless semiconductor where the electrons are considered nearly free as described by the Drude model. When losses due to the electron collisions are taken into account then frequencies close to f_{res} are prohibitively lossy as this frequency corresponds to the extraordinary wave resonance of the semiconductor.

The ideal circulation conditions for regions where the ϵ_{eff} is negative and $|\kappa/\varepsilon|$ is between one and two are shown together with the usual solutions in Figs. 4 and 5. Initial investigations indicate these solutions differ from those where $|\kappa/\varepsilon|$ is greater than unity and ϵ_{eff} is positive. This occurs at frequencies between f_C and f_{res} when f_C is greater than f_A.

The circulation conditions for the value of the gyroelectric ratio above unity are important since for certain values of electron density and applied magnetic field, the semiconductor could have values for which κ/ε lies within this range over a relatively broad range of frequencies. In the limit, if the plasma frequency is related to the cyclotron frequency such that $f_p = \sqrt{2\epsilon_r} f_C$ then the minimum value of $|\kappa/\varepsilon|$ is unity. Hence, broadband circulation designs below f_{res} would only be available in accordance with the perfect circulation conditions generated by the modified Bessel function solutions.

IV. Tracking the Perfect Circulation Curves

The theoretical broadband performance with losses indicated in Fig. 6 illustrates the use of such design curves. GaAs material has been assumed with the following parameters at 77 K: [6] and [7] $m_e^* = 0.067 m_o$, $\epsilon_r = 13$, $\mu_e = 200\,000$ cm^2 V^{-1}s^{-1} and assuming $N = 2 \times 10^{14}$ cm^{-3}, and a flux density $B_o = 0.6$ Tesla. The circulator has a 20 dB isolation bandwidth of about 90% from 48–126 GHz. Fig. 7 shows the real and imaginary components of the gyroelectric ratio for the GaAs cooled to 77 K, with $f_A \simeq 60$ GHz. It is prerequisite for circulator design to have the angular cyclotron

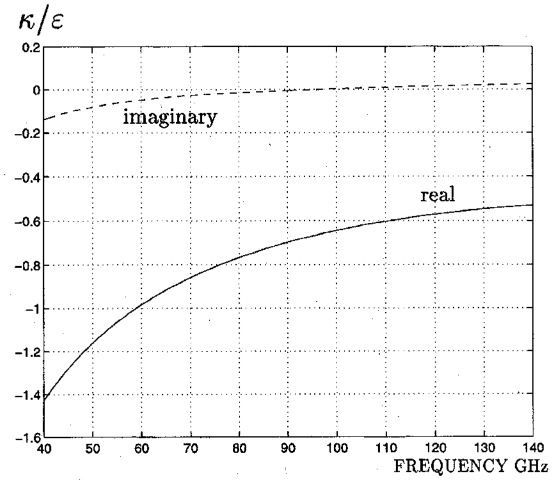

Fig. 7. The gyroelectric ratio of the GaAs junction circulator against frequency. $\epsilon_r = 13$, $B_o = 0.6$ T, $f_{\rm res} = 286$ GHz, and $v_c = 1.3 \times 10^{11}$ s^{-1}.

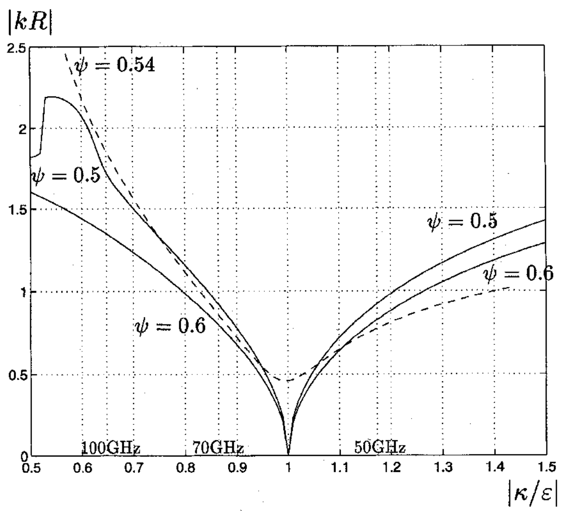

Fig. 8. Tracking behavior of the GaAs junction circulator upon the first circulation condition. — perfect circulation condition; — GaAs circulator design with $R = 0.28$ mm, $\psi = 0.54$ rad, and $\epsilon_d = 20$.

frequency greater than the electron collision frequency, that is $\omega_c > v_c$, for proper interaction between electrons and the electromagnetic fields before random scattering occurs.

In this design, the disk is surrounded by a dielectric of constant $\epsilon_d = 20$, which reduces the impedance ratio $Z_d/Z_{\rm eff}$ by a factor of around 4.5 over the comparable ratio for an air dielectric surround. Careful choice of this dielectric and the half angle, ψ, gives the tracking behavior of this device as shown in Figs. 8 and 9. The device curves presented in these figures differ slightly from those previously depicted in paper [4] because the electron collision frequency is included this time into the expression for $\epsilon_{\rm eff}$ of the GaAs circulator.

It is clear from these figures that the half angle $\psi = 0.54$ radians is a judicious choice. For this value of ψ there is a close correspondence between the ideal performances for $|\kappa/\varepsilon|$ over the range 0.75–0.95. This corresponds to frequencies in the range between 60–80 GHz where the isolation is greater than 30 dB. Another satisfactory tracking region is where $1.05 < |\kappa/\varepsilon| < 1.10$. It is also obvious that these curves do

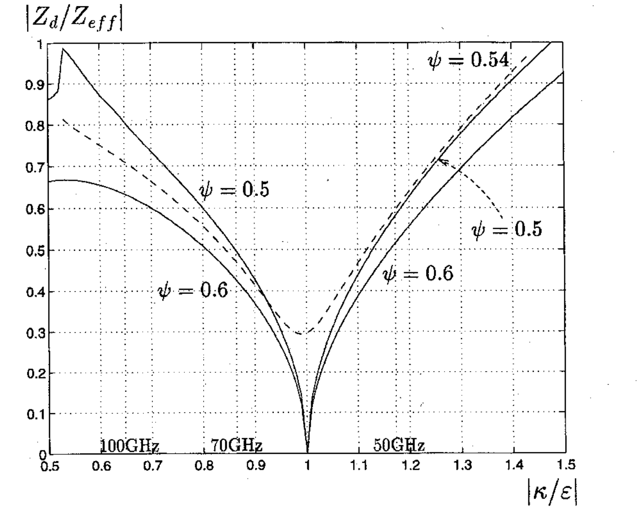

Fig. 9. Tracking behavior of the GaAs junction circulator upon the second circulation condition. — perfect circulation condition; — GaAs circulator design with $R = 0.28$ mm, $\psi = 0.54$ rad, and $\epsilon_d = 20$.

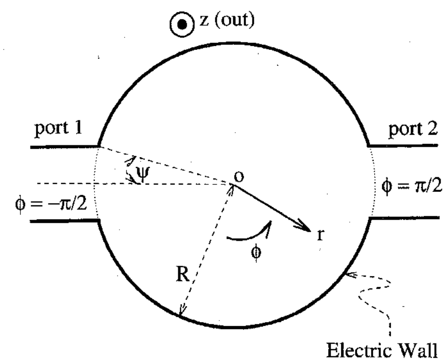

Fig. 10. Schematic diagram of a two-port semiconductor resonator.

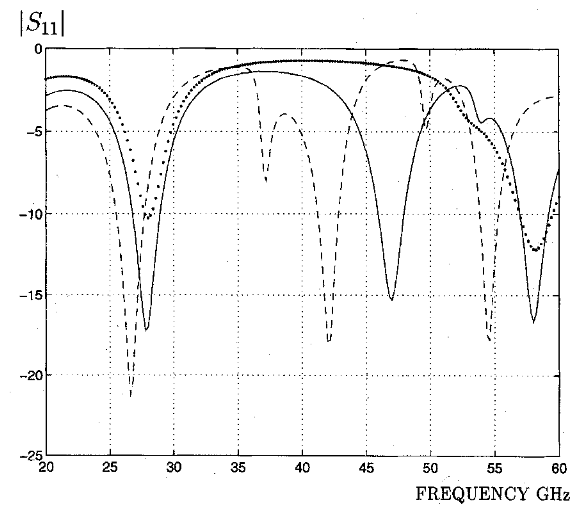

Fig. 11. Theoretical variation of S_{11} of a two-port InSb resonator with frequency for various applied magnetic field. ··· $B_o = 0.4$ T; — $B_o = 0.6$ T; — $B_o = 0.8$ T.

not rapidly diverge for frequencies in close proximity to these ranges of values. Curve tracking is therefore also feasible for $|\kappa/\varepsilon|$ greater than unity for broadband devices at millimetric wavelengths. It is not clear from this theory what the optimum disk thickness is, except that it should be thin enough to avoid overmoding in the disk caused by axial field variation.

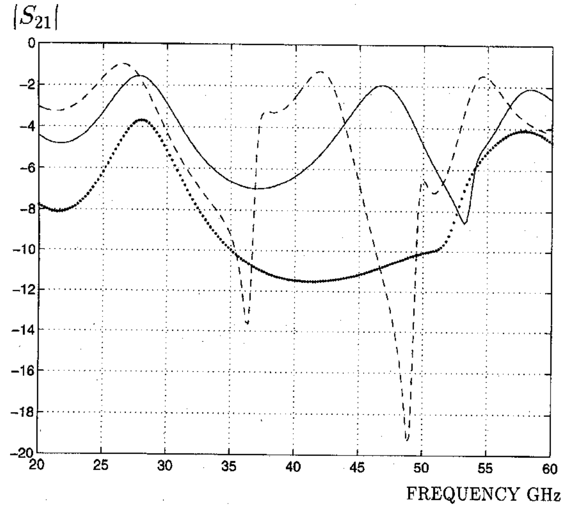

Fig. 12. Theoretical variation of S_{21} of a two-port InSb resonator with frequency for various applied magnetic field. $\cdots$ $B_o = 0.4$ T; — $B_o = 0.6$ T; — $B_o = 0.8$ T.

V. Two-Port Resonator

Although the predicted performance of the design above is satisfactory, it can not be implemented immediately because the accuracy of the semiconductor data available is not known. In order to calibrate any prospective semiconductor material at microwave frequencies and to validate the Drude model, a resonator approach is proposed. The S-parameter response versus frequency for changes in the applied magnetic field will help characterize the semiconductor.

The schematic diagram of the resonator is shown in Fig. 10. The disk architecture is similar to that of the circulator except it has only two ports and each of the ports subtend an angle of 30°. Due to their similar structures, the Green's function analysis of the gyroelectric circulator is applicable in this case and therefore the S-parameters of this two-port network are

$$S_{11} = \frac{Y_d^2 - \overline{G}_1^2 + \overline{G}_2^2}{Y_d^2 - 2Y_d\overline{G}_1 + \overline{G}_1^2 - \overline{G}_2^2} \tag{9}$$

$$S_{21} = \frac{2Y_d\overline{G}_2^2}{Y_d^2 - 2Y_d\overline{G}_1 + \overline{G}_1^2 - \overline{G}_2^2} \tag{10}$$

where Y_d is the slotline admittance. $\overline{G}_1$ and $\overline{G}_2$ are given according to the expressions $\overline{G}_1 = \overline{G}(\pi/2, \pi/2)$ and $\overline{G}_2 = \overline{G}(\pi/2, -\pi/2)$, respectively.

The theoretical S-parameter response of an indium antimonide (InSb) resonator for various values of applied magnetic field, B_o, are illustrated in Figs. 11 and 12. It is clear that the resonances shift with variations in the applied magnetic field. A future paper will comment upon the outcome of these experiments.

VI. Summary

The broadband tracking behavior of the gyroelectric junction circulator has been demonstrated. According to the Drude model of semiconductors, gallium arsenide potentially possesses the low-loss properties necessary to facilitate broadband microwave circulation. A GaAs design is presented which has a 20 dB isolation bandwidth of 90% at a center frequency of 87 GHz and an insertion loss of 1 dB when operated at a temperature of 77 K.

For values of gyroelectric ratio $|\kappa/\varepsilon|$ greater than unity, curves for the perfect circulation conditions are presented. These correspond only to the two frequency regions where the effective permittivity, ϵ_{eff}, is negative. Curve tracking is demonstrated between the perfect circulation curves and the lossy design curve. Only losses due to electron collisions are considered. In the design given, a surrounding dielectric material is assumed of dielectric constant $\epsilon_d = 20$. Careful choice of this material will enable the designer to overlap the perfect circulations and the design curves. The perfect circulation curve lying closest to the design curve gives the optimum value of coupling angle, 2ψ, at the chosen radius for maximum bandwidth performance. The design considered here is at frequencies below the extraordinary wave resonance frequency, f_{res}, but the circulation curves could equally be applied above this resonance.

Finally, in order to calibrate the semiconductor material for practical purposes, a two-port description is given of the junction architecture. Again, this follows the Green's function analysis used to describe the three-port case.

References

[1] Y. S. Wu and F. J. Rosenbaum, "Wide-band operation of microstrip circulators," *IEEE Trans. Microwave Theory Tech.*, vol. MTT-22, pp. 849–856, Oct. 1974.

[2] E. Schloemann and R. E. Blight, "Broad-band stripline circulators based on YIG and Li–Ferrite single crystals," *IEEE Trans. Microwave Theory Tech.*, vol. MTT-34, pp. 1394–1400, Dec. 1986.

[3] L. E. Davis and R. Sloan, "Predicted performance of semiconductor junction circulators with losses," *IEEE Trans. Microwave Theory Tech.*, vol. MTT-41, pp. 2243–2247, Dec. 1993.

[4] R. Sloan, C. K. Yong, and L. E. Davis, "Broadband millimetric semiconductor junction circulators at 77 K," in *IEEE Int. Microwave Symp. Dig.*, San Francisco, CA, June 1996, vol. 1, pp. 109–112.

[5] H. Bosma, "On stripline Y-circulation," *IEEE Trans. Microwave Theory Tech.*, vol. MTT-12, pp. 61–72, Jan. 1964.

[6] M. Sze, *Physics of Semiconductor Devices*. Wiley, 1981, 2nd ed.

[7] O. Madelung, Ed., *Landolt—Bornstein: Numerical Data and Functional Relationships in Science and Technology, Group III: Crystal and Solid State Physics, Vol. 17: Semiconductors, Subvolume a: Physics of Group IV Elements and III–V Compounds*. Berlin/Heidelberg, Germany: Springer-Verlag, 1982.

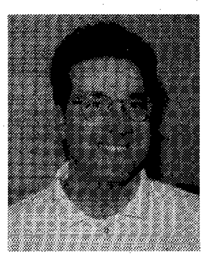

Robin Sloan (M'93) received the B.Sc. degree in electronic engineering from Sussex University, England, in 1985. He then received the M.Sc. degree in communication engineering and digital electronics and the Ph.D. degree from the University of Manchester Institute of Science and Technology (UMIST) in 1988 and 1991, respectively.

From 1985 to 1987, he was with British Aerospace Air Weapons Division, Hatfield, England. From 1991 to 1992, he worked on stripline power combiners at Milmega Ltd., England. Then after a year as a research associate at UMIST, he worked at Ferranti Microwave Ltd, Poynton, England, developing a range of dielectric resonator oscillators. Since June 1994, he has been employed at UMIST as a lecturer in the Applied Electronics Group. His research interests include novel semiconductor devices using magnetoplasmons, electromagnetic field modeling, low-phase noise oscillators, filters, and nonlinear effects in microwave circuits.

Chin K. Yong was born in Johor, Malaysia, on April 26, 1970. He received the B.Eng. degree with First Class Honors in electronic and optoelectronic engineering in 1994 from the University of Manchester Institute of Science and Technology (UMIST), Manchester, UK. He received the M.Sc. degree in 1996.

He is currently a research student at UMIST. His research interests are in gyrotropic components, especially gyroelectric junction circulator.

Lionel E. Davis (F'95) received the B.Sc. and Ph.D. degrees from the University of Nottingham and the University of London in 1956 and 1960, respectively.

From 1959 to 1964, he was with Mulland Research Laboratories, Redhill, England, and from 1964 to 1972, he was an Assistant Professor and then Associate Professor of Electric Engineering at Rice University, Houston, TX. From 1972 to 1987, he was with Paisley College, Scotland, where he was Head of the Department of Electrical Engineering and Electronics and, for two periods, Dean of Engineering. In 1987, he joined the University of Manchester Institute of Science and Technology (UMIST), where he is Professor of Communication Engineering. He has been a Visiting Professor at University College London (1970 to 1971) and the University of California at San Diego (1978 to 1979) and a Consultant for Bendix Research Laboratories (1966 to 1968). His current research interests are in nonreciprocal components, gyrotropic media, high-Tc superconductors, and novel dielectric materials.

Dr. Davis has served on the Council and other committees of the Institution of Electrical Engineering and on several subcommittees of the Science and Engineering Research Council. He was a founding member of the Houston Chapter of the Microwave Theory and Techniques Society. He is a Fellow of the Institute of Electrical Engineers and of the Institute of Physics.